nature portfolio

Peer Review File

Metasurface-Enhanced Mid-Infrared Imaging Spectroscopy with Broadband Quantum Cascade Lasers

Corresponding Author: Dr Ivan Sinev

This file contains all reviewer reports in order by version, followed by all author rebuttals in order by version.

Version 0:

Reviewer comments:

Reviewer #1

(Remarks to the Author)
The authors present a mid-IR spectrometry method using a single RF-modulated QCL, operated to generate frequency components across a 250 cm-1 range, and a diffractive element to spatially separate the laser-generated frequency components. This enables imaging-based spectral correlation across the IR camera pixels. Moreover, the authors employ a gradient metasurface to enhance absorbance signals from thin polymer layers. The two central claims of the paper are metasurface enhancement to increase analyte detection sensitivity and the use of a broadband mid-IR light source for compact, imaging-based spectroscopy. However, these claims are not entirely supported by the results. First, a 250 cm-1 is not broadband and does not offer more than a standard commercially available external-cavity QCL does. Second, the claimed enhancement in detection sensitivity due to the metasurface is not substantiated by appropriate control measurements. While the idea of using a broadband mid-IR laser in conjunction with gradient metasurfaces is appealing, the laser technology appears not to be ready for this application; thus, the title and abstract of this paper may mislead the broad authorship of Nature Communications. I do not recommend the publication of this paper.
• In the abstract and the fifth paragraph of the introduction, the authors make claims without providing supporting data. For example, they use the term “broadband” (lines 96, 87) without providing a numerical spectral range. They claim “enhanced absorption” (line 101) signatures of analytes, but the results do not show any significant enhancement (figure 2d,e).
• Figure 1 is misleading because: 1) gradient metasurface is not directly illuminated by a broadband light source, there is a crucial diffractive grating that does the spatial wavelength separation, not the metasurface, and the diffractive element is not shown in the illustration. Moreover, the analyte detection results shown in Figure 1 are likely from FTIR measurements, not the new optical setup proposed here.
• In Figure 2a, the metasurface position is not indicated; thus, it is confusing to interpret the results. The optical setup shown in Figure 4a used to collect the results, needs to be presented early in Figure 2.
• The RF modulated QCL’s emission range (~250 cm-1) is not broader than external cavity-QCLs (e.g., MIRCAT by Daylights). Yet, in Mircat, 3-4 EC-QCLs are cascaded to cover the significant portion of the fingerprint range. Thus, calling this method “broadband” is an inflated statement.
• As is evident from the measured spectral datasets (figure 2b, d,e), the acquired spectra are extremely noisy. Given that the unique benefits of mid-IR spectroscopy come from capturing very fine spectral variations, the noisy background renders this approach unfit for real-world applications.
• The proposed approach requires a diffractive element and its critical alignment with the gradient metasurface resonances; thus, the benefits of the imaging-based method compared to widely-used tunable EC-QCLs, with a much broader spectral range, are not evident.
• The authors emphasize in the introduction and abstract that SEIRA enhances molecular absorbance. In Figure 2d and e, the reference spectra collected from polymer films deposited on plain CaF2 (No SEIRA) and metasurface (SEIRA) yield the same absorbance. The benefit of using metasurfaces is not clear, especially because the approach relies on a diffractive element that separates the laser wavelengths spatially.
• In lines 162-164, to emphasize the metasurface enhancement, the authors compare the polymer-coated metasurface spectra with FTIR-acquired transmission mode measurements from polymer-coated CaF2 as controls. This is not appropriate because in their reflection mode measurements, the light-path through the analyte layer is doubled (perhaps more than doubled given the oblique light path).
• Moreover, the comparison of transmission and reflection-based FTIR measurements in Figure 3e and f lacks meaning because the light path doubles in reflection mode. What is more concerning is that the authors derive conclusions in lines 168-169 stating 6-times signal enhancement. In the transmission mode measurements of PMMA in Figure 3e, metasurface

resonance blocks light from reaching the FTIR detector, operating the instrument at its poor photon-starved state. The analyte absorbance signal interpretation collected in transmission mode on a reflective metasurface should not be used as a control to demonstrate the SEIRA effect.
• In Figure 5, where the authors quantify the SEIRA effect, they compare the absorption from the proposed laser-based setup with metasurfaces coated with polymer with that of gold mirror measurements on FTIR. This is not an acceptable way to compare signal amplification originating from metasurface resonances collected on two different substrates and instruments with distinct optical light-paths.
• To prove their claims about the SEIRA based signal enhancement and the need for a gradient metasurface in the proposed optical configuration, the authors must compare their polymer layer coated metasurface measurements with the following controls on the same optical setup shown in Figure 4a: 1) by coating the diffraction grating with the same thickness of PMMA and extracting absorbance without the metasurface (or metasurface replaced with a gold mirror in Figure 4a). 2) by replacing the PMMA-coated metasurface with an Au mirror substrate coated with an identical thickness of PMMA and measuring spectra on the same setup Figure 4a). 3) In the setup in Figure 4a, keeping a bare metasurface in place and by inserting a PMMA coated CaF2 on the light path before the camera. Comparing measured spectra from these three control measurements with the PMMA coated metasurface and showing significant signal enhancement can prove the SEIRA effect in this setup.
• The methods for the fabrication of the metasurface are not sufficient for the readers to reproduce the results. Clarifications are needed on why an inverted pattern was exposed using EBL instead of using a negative resist or a positive resist with a hard mask to etch Ge. Also, details on Ge etching recipe (gas type, flow rate, plasma power) need to be included.

Reviewer #3

(Remarks to the Author)
The paper reports on an advanced SEIRA technique with pronouncedly reduced acquisition time. Such a breaking result was obtained with the use of a few crucial improvements in the experimental method. First, a quantum cascade laser with radio-frequency modulation provides a broadband coherent source for mid-IR spectrometry. Second, a metasurface helps to enhance the response. Third, the gradient variation of the lattice constant of the metasurface elements allows for achieving a frequency range translation in the coordinate space. All these actions lead to an extremely short time of the Mid-IR acquisition, validated experimentally with reasonable accuracy. Thus, the paper, which presents a novel trustworthy experimental spectroscopy technique, warrants publication. However, there are a few points that require attention to better convey the results to the auditorium.
Comments.
1. It is not clear how the absorption spectra were extracted, taking into account that reflection is measured in the range of 0 to 0.6. Is it simply the reflection of a bare metasurface minus the reflection of a metasurface coated with an analyte layer? Did the analyte coating happen from the substrate part or on top of the metasurface elements? What about the analytes' profile then? It will be nice to provide a more detailed description of the retrieval of infrared absorption.
2. The small red arrow in Fig.3e is hardly visible, however, the clearly seen red curve is not explained in the Caption.
3. It is worth showing the main fingerprints of the analyte vibration bands used for the method characterisation directly in Fig.5d-i (also Fig.2d,e) but not referring to them in the bold text.
4. Have the FTIR spectra in Fig.2d,e, error bars, or are they too small to be seen? Should be commented.
5. While blue and red curves in Fig.5g-i are matching pretty well in the range1425 -1500 cm^-1, QCL SEIRA provides additional features beyond this range. These features are not supported by FTIR measurement despite its very small errors according to the calibration in Fig.2. Are there any explanations?

Version 1:

Reviewer comments:

Reviewer #1

(Remarks to the Author)
I thank the authors for clarifying the advantages of their laser source in the context of infrared spectroscopy. With these revisions, the manuscript now positions its contribution more clearly within the field. I would still encourage the authors to avoid potentially exaggerated wording such as “… remarkably broad …” and instead adopt more objective and quantitative language throughout the text.

Given that the principal strength of the proposed method appears to be its acquisition speed (reported to be approximately three orders of magnitude faster than FTIR), it would be valuable for the authors to discuss in more detail which sensing or spectroscopy applications critically benefit from such speed. Highlighting specific use cases where this performance advantage is essential would further strengthen the motivation and impact of the work.

Reviewer #3

(Remarks to the Author)
The reviewer's comments elicited a quite verbose response letter with intensive discussions on many important points. The answers and changes made in the revised manuscript definitely improve the quality and readability of the paper and the trustworthiness of the presented results. The paper warrants publication in the journal.

Reviewer #1 (Remarks to the Author):

The authors present a mid-IR spectrometry method using a single RF-modulated QCL, operated to generate frequency components across a 250 cm-1 range, and a diffractive element to spatially separate the laser-generated frequency components. This enables imaging-based spectral correlation across the IR camera pixels. Moreover, the authors employ a gradient metasurface to enhance absorbance signals from thin polymer layers. The two central claims of the paper are metasurface enhancement to increase analyte detection sensitivity and the use of a broadband mid-IR light source for compact, imaging-based spectroscopy. However, these claims are not entirely supported by the results. First, a 250 cm-1 is not broadband and does not offer more than a standard commercially available external-cavity QCL does. Second, the claimed enhancement in detection sensitivity due to the metasurface is not substantiated by appropriate control measurements. While the idea of using a broadband mid-IR laser in conjunction with gradient metasurfaces is appealing, the laser technology appears not to be ready for this application; thus, the title and abstract of this paper may mislead the broad authorship of Nature Communications. I do not recommend the publication of this paper.

We appreciate the Reviewer's positive feedback on our concept ("the idea of using a broadband mid-IR laser in conjunction with gradient metasurfaces is appealing") and constructive suggestions that helped us improve the manuscript. However, we cannot agree with Reviewer's main criticism regarding the qualities of our QCL as well as with his/her claim that the laser technology is not ready for the application. First, we would like to stress that our QCL has a unique edge as it provides **instantaneous** broad emission spectrum, i.e. all spectral components are emitted within a single pulse. This feature is in strong contrast to the external cavity QCLs (EC-QCLs) that the Reviewer is referring to because EC-QCLs are inherently **narrowband light** sources. Extended spectral coverage of EC-QCL systems is achieved by mechanical tuning of the cavity, which limits the operation speed, and brings additional issues of instability. For example, commercially available Mircat from Daylight Solutions has a reported step-and-settle time of 250 ms (https://www.daylightsolutions.com/products/mircat/).
In this context, our broadband laser should rather be compared to frequency combs that also provide instantaneously broad spectrum, but combs have much narrower emission bands of several tens of cm-1. Only some research grade state-of-the-art solutions reached ~100 cm-1. Thus, the RF-modulated QCL that we implement in our manuscript has a unique advantage in terms of providing a remarkably broad band instantaneous emission spectrum. Importantly, this feature combined with broadband metasurfaces allowed us to demonstrate for the first time fast detection of molecular absorption barcodes in a single frame with a low-cost and room-temperature mid-IR camera, and reduce the acquisition time by up to 3 orders of magnitude compared to the FTIR and EC-QCL based measurements.

We also would like to reiterate that a 250 cm-1 wide spectral band (centered at ~1460 cm-1) is very broad for performing spectroscopy analysis because it covers a molecular fingerprint-rich range with many characteristic vibrational bands, which allows discrimination between multiple distinct molecular species.

ACTIONS TAKEN:

We revised the abstract and introduction considerably to clarify the ambiguous points mentioned by the Reviewer and highlight the advantages of our system that enable the rapid detection of absorption signatures.

The revised abstract now reads:

Mid-infrared (mid-IR) spectroscopy offers unparalleled opportunities in sensing through chemically specific detection of molecular absorption fingerprints. Yet, its practical applications are limited by the weak light-matter interaction in the mid-IR range and low brightness of mid-IR light sources. Surface-enhanced infrared absorption (SEIRA) spectroscopy addresses the sensitivity limitations by leveraging resonant photonic structures, in particular, plasmonic and frequency-selective dielectric metasurfaces. However, current implementations of SEIRA approach mainly rely on complex instruments and scanning components such as Fourier-transform infrared spectroscopy and tunable ~~lasers~~external cavity quantum cascade lasers (EC QCLs). Here, we present a compact ~~,~~ and high-throughput imaging-based SEIRA platform that combines ~~a broadband ,~~ broadband gradient metasurfaces with a radiofrequency-modulated ~~quantum cascade laser (QCL) with gradient metasurfaces supporting resonances over a wide spectral range. Their synergistic combination in an imaging-based architecture enables spatially resolved single-frame acquisition of molecular absorption fingerprints without any laser scanning or mechanically moving parts~~QCL that generates remarkably broad instantaneous emission spectrum (250 cm^{-1}) covering absorption bands of multiple distinct molecular vibrational modes. By matching the resonance spectrum of the compact (1 mm^2) broadband gradient metasurface with the ~~dispersion of the broadband QCL~~ laser emission projected on ~~the sample surface , we realize imaging based~~ its surface through a dispersive element, we ensure that every QCL spectral component is uniquely addressed for an efficient targeted enhancement of the electromagnetic field. This enables us to use a low-cost and room-temperature mid-IR ~~absorption detection in a 1 mm^2 device footprint using a room temperature mid IR imaging camera with acquisition time more than~~ camera, acquiring in a single frame the enhanced absorption signatures of analytes deposited on the metasurface as a barcode image, thus reducing the acquisition time by up to 3 orders of magnitude ~~shorter than FTIR-based~~ compared to the FTIR and EC QCL based measurements. Eliminating the need for tunable light sources, bulky spectrometers, and expensive low-temperature detectors, our approach enables high-throughput, miniaturized, and highly specific molecular diagnostics for diverse chemical and biological applications.

The revised introduction now reads:

The development of quantum cascade lasers (QCLs) presents a promising alternative to traditional mid-IR sources. ~~QCLs offer~~ QCL is normally a narrowband (few MHz linewidth) source offering high-intensity, coherent radiation, which significantly improves the spectral resolution and simplifies the detection. Given the importance of broadband mid-IR spectroscopy, QCL architectures that ~~provide large emission bandwidth~~ are capable of addressing broader spectral ranges gained particular attention. ~~External~~ State-of-the-art external cavity (EC) QCLs[21, 22] were able to reach ~~bandwidths~~ tuning ranges of up to several hundreds of cm^{-1} ~~by heterogeneous integration of several cascade designs in a single active region~~with mechanically scanned components[23]. Combination of tunable EC QCLs with pixelated SEIRA metasurfaces that provide spatially encoded spectral information facilitated a shift toward spectrometerless, imaging-based mid-IR characterization techniques[18, 20, 24].

However, the use of EC still entails extended acquisition times dictated by the moving parts of the laser tuning system, which also require a higher degree of mechanical stability of the system and in general a larger setup footprint [34]. Frequency comb (FC) QCLs[25] ~~have emerged recently as another promising candidate for broadband~~ differ from the EC QCL by the fact that they provide instantaneous broad spectrum. As a result, they have recently emerged as a promising on-chip and compact source to perform rapid mid-IR ~~spectroscopy~~analysis over a large spectral band. In particular, ~~double-comb~~ dual-comb spectroscopy techniques offer short (μs) acquisition times and no moving parts[26], significantly improving the measurement reliability. While the FC bandwidth is typically limited to ~ 100 cm^{-1}[27, 28], it was recently proven that a ~~broader spectral coverage of QCLs can be achieved through a~~ strong radio-frequency modulation ~~. This~~ of a narrowband QCL can result in a remarkably broader spectral coverage. This modulation drives the device to operate in a quasi-coherent regime, where the typical linewidth of the laser is of the order of the modulation frequency [29] (hundreds of MHz) ~~, which makes it~~ and the full spectrum is emitted in a single laser pulse. Importantly, with this approach it is possible to use the same active material employed in tunable EC-lasers but without requiring any moving parts and mechanical stabilization, which results in a platform that is highly appealing for broadband spectroscopy, including SEIRA.

In this paper, we propose a rapid imaging-based SEIRA spectroscopy technique enabled by the synergistic combination of ~~a broadband QCL operating under RF modulation and broadband~~ broadband resonance gradient metasurfaces and an RF-modulated QCL generating remarkably broad instantaneous emission spectrum over 250 cm^{-1} (Fig. 1). In our measurement configuration, we match the local resonance of a compact (footprint ≈ 1 mm^2) gradient metasurface with the spectral dispersion of the laser radiation projected on it ~~, providing~~ for efficient targeted enhancement of the electromagnetic field~~in the full emission range . The~~ . The broad emission range of our laser simultaneously covers absorption bands of multiple distinct molecular vibrational modes without any time-consuming mechanical tuning that is required in conventional EC QCL systems. This allowed us to use a low-cost and room-temperature mid-IR imaging camera to capture in a single frame the enhanced absorption signatures of analytes deposited on the gradient chip ~~are captured in a barcode-like format in a single frame of a low-cost, room-temperature mid-IR imaging camera. With the spectral range of our device covering the absorption bands of several distinct molecular vibrational modes, we~~ as a barcode image, improving the detection time by up to 3 orders of magnitude as compared to FTIR and EC QCL based systems. We envision the use of our approach for rapid and specific diagnostics of diverse chemical compounds, leading to compact and low-cost mid-IR sensors for operation ~~at~~ in remote settings.

We further highlighted the main advantages of our work towards conclusion:

~~In addition to the strong absorption signal~~ Empowered by the spatially-resolved SEIRA enhancement, our platform provides ~~unparalleled~~ a decisive advantage over conventional mid-IR spectroscopy techniques in terms of acquisition speed. All presented ~~imaging SEIRA data are~~ BQCL barcode data were captured at 7 fps readout (14 ms per frame) with a room temperature mid-IR camera. This represents a 3 orders of magnitude improvement over the FTIR measurements of thin films without SEIRA enhancement (blue lines in Fig. 5g-i, ~~120s~~ 3 minutes per measurement)~~and up to 4 orders improvement as compared to~~ . This difference is even more pronounced for FTIR SEIRA measurements that ~~also involve~~ require mechanical scanning of the collection area along the gradient chip (Fig. 5a-c~~,~~), bringing the total detection time to 20 min per measurement ~~). This~~ (4 orders of magnitude difference with single-shot BQCL data). Similarly, due to instantaneously broad emission spectrum of our QCL, it excels over the commercial EC-QCL systems that require mechanical wavelength scanning (Fig. 3d took 20 s for to cover the full spectral range of BQCL). Therefore, our approach represents a breakthrough advancement for high-throughput, highly sensitive molecular diagnostics in mid-IR.

- **In the abstract and the fifth paragraph of the introduction, the authors make claims without providing supporting data. For example, they use the term "broadband" (lines 96, 87) without providing a numerical spectral range. They claim "enhanced absorption" (line 101) signatures of analytes, but the results do not show any significant enhancement (figure 2d,e).**

We appreciate the Reviewer's remarks. We revised the abstract and introduction to specify the emission band of our QCL (250 cm-1) and compare it against state-of-the-art mid-IR sources. Please see our response to the previous comment for an extended explanation about the broadband feature.

Regarding the enhancement, we would like to clarify that the quantification analysis of the absorption enhancement of the analyte from our gradient metasurface is provided exclusively in Fig. 5. In fact, the data shown in Fig. 2 demonstrates QCL-based imaging spectroscopy on thick polymer films **without the use of the metasurface**, and therefore does not contain any SEIRA-type amplification. To make this point more clear for the reader, we revised the figure caption and specified that this Figure represents **non-enhanced** imaging spectroscopy.

ACTIONS TAKEN:

We revised Fig.2 and its caption to clarify that the presented data corresponds to the imaging spectroscopy without SEIRA enhancement and therefore should not be considered as confirmation of metasurface-enhanced absorption. We also changed the color coding of the BQCL data to avoid the confusion with the FTIR spectrum shown in Fig. 2b.

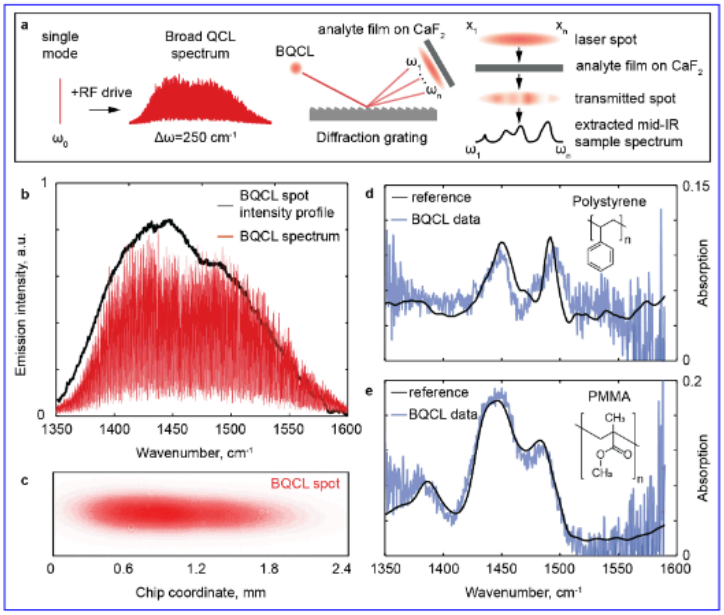

Figure 2 ~~Imaging spectroscopy with broadband quantum cascade laser~~ Non-enhanced imaging spectroscopy with broadband quantum cascade laser (a) Schematic of the broadband QCL imaging spectroscopy components. Left: quantum cascade laser is driven into broadband emission regime using radiofrequency drive. Center: broadband laser emission is projected on a sample surface (here, thin polymer films on CaF^2 chips) through a dispersive element and then imaged with a mid-IR camera. Right: as each frequency component of BQCL addresses a specific coordinate on the sample surface, the spatial profile of the laser spot represents the sample transmission spectrum~~that can be extracted from a single frame of a mid-IR imaging camera~~. (b) Spatial intensity profile of a projected laser spot (black curve) compared to the spectrum of BQCL emission measured with FTIR (red curve). (c) Image of the BQCL spot on the surface of CaF_2 chip recorded with a mid-IR camera. (d,e) Comparison of the absorption spectra of (d) polystyrene and (e) polymetylmetacrylate films on CaF_2 measured with FTIR (black curves, smoothed using a 20-point moving average) and extracted from the spatial intensity profiles of the transmitted BQCL beam (~~red~~ blue curves).

- **Figure 1 is misleading because: 1) gradient metasurface is not directly illuminated by a broadband light source, there is a crucial diffractive grating that does the spatial wavelength separation, not the metasurface, and the diffractive element is not shown in the illustration. Moreover, the analyte detection results shown in Figure 1 are likely from FTIR measurements, not the new optical setup proposed here.**

We thank the Reviewer for pointing out the ambiguity. Following the Reviewer's advice, we added the diffraction grating in the revised schematic. The analyte detection results indeed are from FTIR, however, we find it important to include the FTIR spectra to illustrate the mechanism behind the manifestation of the reflectivity profile of resonance gradient metasurfaces covered with the analyte.

ACTIONS TAKEN:

To ensure that Figure 1 is not misleading for the reader and does not miss important components of the setup, we revised it by adding the diffraction grating to the device schematic. We also added the real data measured in the imaging configuration with BQCL setup to the schematic on the right. Furthermore, we revised the caption to ensure that the reader interprets the presented spectra correctly.

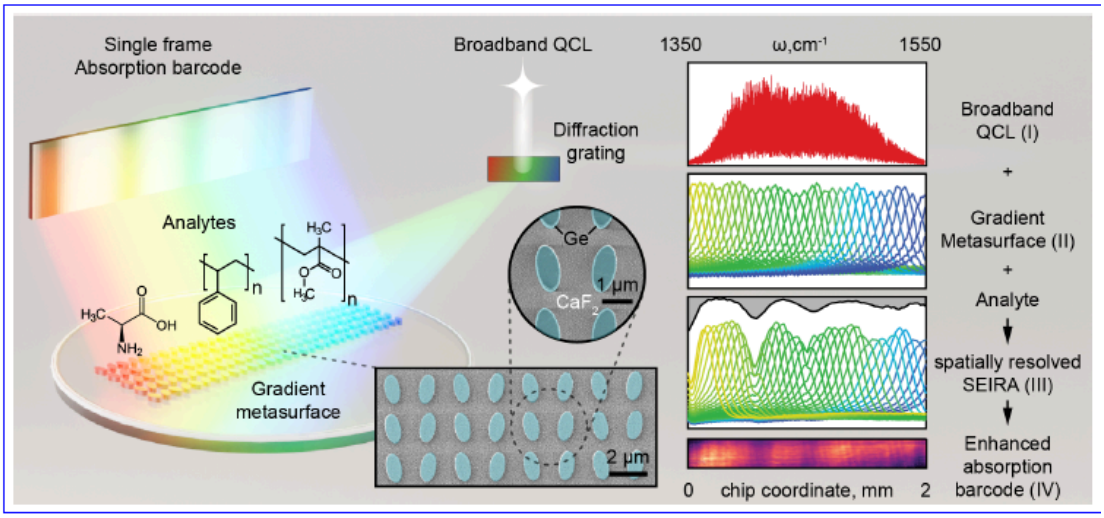

Figure 1 ~~Illustration of rapid SEIRA-based imaging spectroscopy enabled by broadband QCL augmented with resonance gradient metasurfaces.~~ ~~Broadband QCL~~ Illustration of rapid imaging-based SEIRA spectroscopy enabled by the synergy of resonance gradient metasurfaces and RF-modulated QCL generating broad instantaneous emission spectrum. Left: laser emission is projected on the metasurface through a dispersive element, providing spatially resolved SEIRA signal. The gradient of the metasurface resonance is tailored to match the spectral component of the broadband laser addressing each location on the chip. The reflectivity of the resonance gradient metasurface is then captured in a single frame of a room-temperature mid-IR imaging camera, allowing to detect the absorption signature of analytes deposited on the metasurface in a barcode-like format. The insets show the false color SEM images of the gradient metasurface. Right: Broad QCL spectrum (I) is matching the spectral coverage of the resonance gradient metasurface, represented here with a stack of spatially resolved reflectivity spectra measured with FTIR (II). Deposition of analyte on the metasurface leads to local modifications of the resonant peaks where their spectral position overlaps with analyte absorption peaks (III). This yields spatial variations of reflectivity of BQCL spot, which is recorded in the form of unique absorption barcode (IV).

- **In Figure 2a, the metasurface position is not indicated; thus, it is confusing to interpret the results. The optical setup shown in Figure 4a used to collect the results, needs to be presented early in Figure 2.**

We thank the reviewer for bringing up this point and allowing us to make the text more clear. As mentioned above, Fig. 2 demonstrates the results of the broadband QCL imaging spectroscopy on **bare CaF2 chips,** such that without the metasurface and the associated absorption signal enhancement. These data are intended to illustrate the imaging aspect of the proposed configuration and to highlight that when our mid-IR source providing **simultaneous** broadband emission is coupled with a room-temperature IR camera, it can be used for rapid characterization of thick IR-absorptive films. To ensure the reader interprets the content of Fig. 2 correctly, we revised the caption to draw attention that it is the non-enhanced spectroscopy technique that is being illustrated.

ACTIONS TAKEN:
We revised the caption of Fig. 2 (see our response above) as well as the related text in the main manuscript to ensure that the reader does not miss the fact that Fig. 2 discusses the non-enhanced version of imaging spectroscopy:

The emission band of the chosen BQCL device ($1350 - 1600\ \mathrm{cm}^{-1}$) covers a spectral region extremely rich in signatures of vibrational modes of organic molecules, including vinyl C-H bends, aromatic ring stretch modes, carboxyl group modes, and more[31]. The transmission configuration described above can be used ~~to detect~~ for rapid detection of the absorption spectra of relatively thick layers of analytes without SEIRA enhancement. We showcase this for films of ~~Polystyrene~~ polystyrene

- **The RF modulated QCL's emission range (~250 cm-1) is not broader than external cavity-QCLs (e.g., MIRCAT by Daylights). Yet, in Mircat, 3-4 EC-QCLs are cascaded to cover the significant portion of the fingerprint range. Thus, calling this method "broadband" is an inflated statement.**

We cannot agree with the reviewer on this specific point. As we already argued in the first comment above, our RF-driven QCL gives a unique edge by providing an **instantaneously** broad emission spectrum. This is a critical factor for rapid absorption detection that we demonstrate in this work. Quite contrary, EC QCLs are inherently narrowband (few MHz) light sources, for which mechanical tuning of the external cavity is required to cover extended spectral ranges. This also means additional time is needed to switch between the channels in cascaded configurations like the one mentioned by the Reviewer. In fact, in the original version of the manuscript we already compared the acquisition time of our setup with Daylight Solutions Spero QCL-based microscope (housing 4 separate MIRCAT EC-QCLs), which takes ~ 1 minute to do the wavelength sweep and requires additional data post-processing to extract the absorption barcode. We also point out that in our application, a 250 cm-1 emission band (centered at ~1460 cm-) is broad to cover a spectral range particularly rich with molecular fingerprints, which allows discrimination between distinct analyte species.

Importantly, this work demonstrates for the first time fast detection of molecular absorption barcodes in an important spectral range by capturing the fingerprint information in a single frame with a low-cost and room-temperature mid-IR camera, and reports up to 3 orders of

magnitude reduced acquisition time in comparison to the state-of-the-art EC-QCL based measurements.

ACTIONS TAKEN:
We revised the introduction of our manuscript to include the clarification of this unique feature of our laser. We also added the discussion on the decisive advantages of having an instantaneously broad spectrum vs. external cavity solutions that require mechanical tuning of the cavity.

The development of quantum cascade lasers (QCLs) presents a promising alternative to traditional mid-IR sources. ~~QCLs offer~~ QCL is normally a narrowband (few MHz linewidth) source offering high-intensity, coherent radiation, which significantly improves the spectral resolution and simplifies the detection. Given the importance of broadband mid-IR spectroscopy, QCL architectures that ~~provide large emission bandwidth~~ are capable of addressing broader spectral ranges gained particular attention. ~~External~~ State-of-the-art external cavity (EC) QCLs[21, 22] were able to reach ~~bandwidths~~ tuning ranges of up to several hundreds of cm^{-1} ~~by heterogeneous integration of several cascade designs in a single active region~~with mechanically scanned components[23]. Combination of tunable EC QCLs with pixelated SEIRA metasurfaces that provide spatially encoded spectral information facilitated a shift toward spectrometerless, imaging-based mid-IR characterization techniques[18, 20, 24].

However, the use of EC still entails extended acquisition times dictated by the moving parts of the laser tuning system, which also require a higher degree of mechanical stability of the system and in general a larger setup footprint [34]. Frequency comb (FC) QCLs[25] ~~have emerged recently as another promising candidate for broadband~~ differ from the EC QCL by the fact that they provide instantaneous broad spectrum. As a result, they have recently emerged as a promising on-chip and compact source to perform rapid mid-IR ~~spectroscopy~~analysis over a large spectral band. In particular, ~~double comb~~ dual-comb spectroscopy techniques offer short (μs) acquisition times and no moving parts[26], significantly improving the measurement reliability. While the FC bandwidth is typically limited to ~ 100 cm^{-1}[27, 28], it was recently proven that a ~~broader spectral coverage of QCLs can be achieved through a~~ strong radio-frequency modulation ~~. This~~ of a narrowband QCL can result in a remarkably broader spectral coverage. This modulation drives the device to operate in a quasi-coherent regime, where the typical linewidth of the laser is of the order of the modulation frequency [29] (hundreds of MHz) ~~, which makes it~~ and the full spectrum is emitted in a single laser pulse. Importantly, with this approach it is possible to use the same active material employed in tunable EC-lasers but without requiring any moving parts and mechanical stabilization, which results in a platform that is highly appealing for broadband spectroscopy, including SEIRA.

- **As is evident from the measured spectral datasets (figure 2b, d,e), the acquired spectra are extremely noisy. Given that the unique benefits of mid-IR spectroscopy come from capturing very fine spectral variations, the noisy background renders this approach unfit for real-world applications.**

We thank the Reviewer for bringing up this point, which gave us the opportunity to perform new measurements and strengthen our paper with the additional data. Firstly, the presented FTIR data used as a reference was smoothed for better visual representation. Secondly, the BQCL data indicates that the noise level is relatively small (see below for quantitative characterization) in the middle of the spectral range and increases towards its edges. This is

explained by decrease of the laser spectral power density towards the edges of its emission spectrum. However, the most important aspect here is that this noise level is achieved for **extremely short detection time** (0.14s) and using a **low-cost room temperature IR camera**. In fact, the FTIR spectrometer, which has a LN-cooled detector instead of room temperature one as in our case, yields considerably higher noise for comparable collection time. Therefore, detection of fine spectral features mentioned by the Reviewer can only be achieved with extended acquisition times. To illustrate this point and quantitatively compare the noise level for FTIR and BQCL data, in the revised Supplementary Materials we present the absorption spectra measured with FITR for different acquisition times. These new experimental results clearly demonstrate superior performance of our imaging spectroscopy setup, with noise level of FTIR improving only for acquisition times over 2 minutes, thus, 3 orders of magnitude difference with the BQCL acquisition time of 0.14 s. Rapid detection capabilities of the BQCL setup can potentially be sacrificed to average over multiple frames of the detector. However, here we capitalize on the faster acquisition time as we consider it to be the main advantage of our configuration.

Lastly, we would like to point out again that the measurement configuration presented in Fig. 2 is indeed not suitable for discrimination of fine (weak) absorption signatures, as it represents data measured without SEIRA aspect. Instead, the configuration with gradient metasurface (discussed in Figs.3-5) should be used to improve the SNR by amplifying weak absorption signatures.

ACTIONS TAKEN:

We added the discussion of the observed noise level to the revised manuscript. We also performed new measurements to illustrate the advantages of our approach for rapid detection of absorption using the PMMA film on CaF2 as a representative example. New data are presented in the Supplementary Information Figure S2 and referenced in the main text as follows:

amplitude and spectral position of the peaks. ~~However, they manifest larger noise , which we attribute mainly to the~~ The main source of the noise in the BQCL spectra is the room-temperature imaging camera utilized in our setup[29]. ~~The increase of noise~~ Lower laser intensity towards the edges of the spectral range ~~is due to smaller laser intensity and thus~~ leads to larger contribution of the detector noise to the normalized signal. Importantly, while BQCL data are recorded in a single snapshot of the camera (140 ms), achieving a comparable noise level in FTIR data requires averaging of the spectra for over 2 minutes (see Supplementary Information Figure S2), which highlights the rapid detection capabilities of our approach.

Revisions in the SI text:

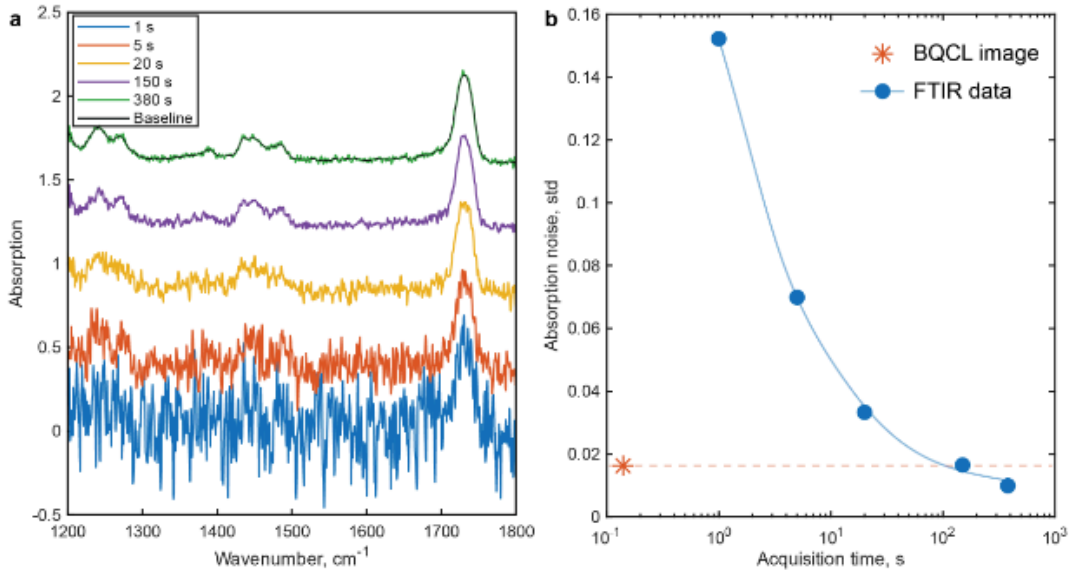

Figure S2: **a**, Absorption spectra of 800 nm PMMA layer on CaF_2 chip measured for different acquisition time (number of averages), illustrating the reduction of noise level with longer measurement. Each consecutive spectrum is shifted vertically by 0.4 to facilitate the comparison. **b,** Dependence of the noise level calculated as the standard deviation from the absorption baseline (shown with black curve on top of 380 s spectrum in panel a).

- **The proposed approach requires a diffractive element and its critical alignment with the gradient metasurface resonances; thus, the benefits of the imaging-based method compared to widely-used tunable EC-QCLs, with a much broader spectral range, are not evident.**

We thank the reviewer for this comment. While alignment is indeed critical in our approach, the advantage is that, unlike in the EC-QCL system, our configuration is stationary, and the whole setup has no mechanically moving parts, which improves the stability. We also stress again that using broadband RF-QCL and gradient metasurfaces enables unique synergy, as every spectral component uniquely addresses the corresponding chip location providing its resonant enhancement. To achieve such functionality with EC-QCL, one would need not only to scan the cavity to tune the wavelength, but also scan the laser spot over the chip surface to address the locations with respective resonant field enhancement.

ACTIONS TAKEN:
We highlighted the advantages of our stationary configuration vs. mechanically tunable EC QCL solutions in the revised Introduction:

and no moving parts[26], significantly improving the measurement reliability. While the FC bandwidth is typically limited to ~ 100 cm^{-1}[27, 28], it was recently proven that a ~~broader spectral coverage of QCLs can be achieved through a~~ strong radio-frequency modulation ~~. This~~ of a narrowband QCL can result in a remarkably broader spectral coverage. This modulation drives the device to operate in a quasi-coherent regime, where the typical linewidth of the laser is of the order of the modulation frequency [29] (hundreds of MHz) ~~, which makes it~~ and the full spectrum is emitted in a single laser pulse. Importantly, with this approach it is possible to use the same active material employed in tunable EC-lasers but without requiring any moving parts and mechanical stabilization, which results in a platform that is highly appealing for broadband spectroscopy, including SEIRA.

- **The authors emphasize in the introduction and abstract that SEIRA enhances molecular absorbance. In Figure 2d and e, the reference spectra collected from polymer films deposited on plain CaF2 (No SEIRA) and metasurface (SEIRA) yield the same absorbance. The benefit of using metasurfaces is not clear, especially because the approach relies on a diffractive element that separates the laser wavelengths spatially.**

We thank the reviewer for bringing up this point and allowing us to address the confusion caused by the data presented in Fig. 2. As described in above comments, in fact there are no SEIRA data in this Figure; instead, the data both in 2d and 2e show absorption data obtained from thick polymer layers on CaF2 in a single-shot with our imaging setup using a simultaneous broadband emission source and a room temperature camera (blue lines) versus an FTIR instrument using a scanning mirror and a cooled single point detector (black lines). Thus, this Figure is intended to highlight the possibility of rapid collection of the absorption signatures of thick films with our imaging setup even without SEIRA enhancement. The new Supplementary Figure S2 discussed above quantifies the advantage of our setup in detection time compared to FTIR.
Consecutively, there is no SEIRA enhancement in any of the spectra presented in Figure 2. Additionally, it is important to clarify that the imaging data are collected within a single snapshot of the camera (14 ms detection time), while the FTIR spectra were averaged for 150 s and smoothed using a 20-point moving average.

ACTIONS TAKEN:
Caption of Fig. 2 was revised to avoid possible confusions.

Figure 2 ~~Imaging spectroscopy with broadband quantum cascade laser~~ **Non-enhanced imaging spectroscopy with broadband quantum cascade laser** (a) Schematic of the broadband QCL imaging spectroscopy components. Left: quantum cascade laser is driven into broadband emission regime using radiofrequency drive. Center: broadband laser emission is projected on a sample surface (here, thin polymer films on CaF^2 chips) through a dispersive element and then imaged with a mid-IR camera. Right: as each frequency component of BQCL addresses a specific coordinate on the sample surface, the spatial profile of the laser spot represents the sample transmission spectrum~~that can be extracted from a single frame of a mid-IR imaging camera~~. (b) Spatial intensity profile of a projected laser spot (black curve) compared to the spectrum of BQCL emission measured with FTIR (red curve). (c) Image of the BQCL spot on the surface of CaF_2 chip recorded with a mid-IR camera. (d,e) Comparison of the absorption spectra of (d) polystyrene and (e) polymetylmetacrylate films on CaF_2 measured with FTIR (black curves, smoothed using a 20-point moving average) and extracted from the spatial intensity profiles of the transmitted BQCL beam (~~red~~ blue curves).

- **In lines 162-164, to emphasize the metasurface enhancement, the authors compare the polymer-coated metasurface spectra with FTIR-acquired transmission mode measurements from polymer-coated CaF2 as controls. This is not appropriate because in their reflection mode measurements, the light-path through the analyte layer is doubled (perhaps more than doubled given the oblique light path).**

We thank the reviewer for bringing out this point and allowing us to clarify the relevant parts . In lines 162-164 of the original manuscript, **we do not discuss the magnitude of SEIRA enhancement** of absorption signatures. Instead, we explain that for our metasurface design, the enhanced absorption signal is contributing predominantly to the modulation of reflectivity. This is done **not to quantify the SEIRA enhancement**, but to justify the change of measurement configuration as compared to Fig. 2. We never use the FTIR-acquired

transmission mode measurements of polymers on CaF2 as controls. Instead, we use the FTIR data shown in Fig. 3e,f to show that the absorption signal of the analyte contributes to the modification of the reflected peak amplitude, while the amplitude of the transmission dip remains mostly unaffected. Since resonant mode excitation is involved, the increased light path is not enough to explain this phenomenon; instead, the balance of radiative and non-radiative loss of the resonance should be taken into account. In particular, the metasurface can be re-designed to ensure that the absorption signal is manifested better in transmission, in direct contradiction to light path considerations (e.g. https://opg.optica.org/optica/fulltext.cfm?uri=optica-12-2-178); however, this is out of scope of our current manuscript.

ACTIONS TAKEN:

We revised the corresponding part of the manuscript to ensure that the purpose of Fig. 3 and related discussion are more clear for the reader. The revised sections now read as follows:

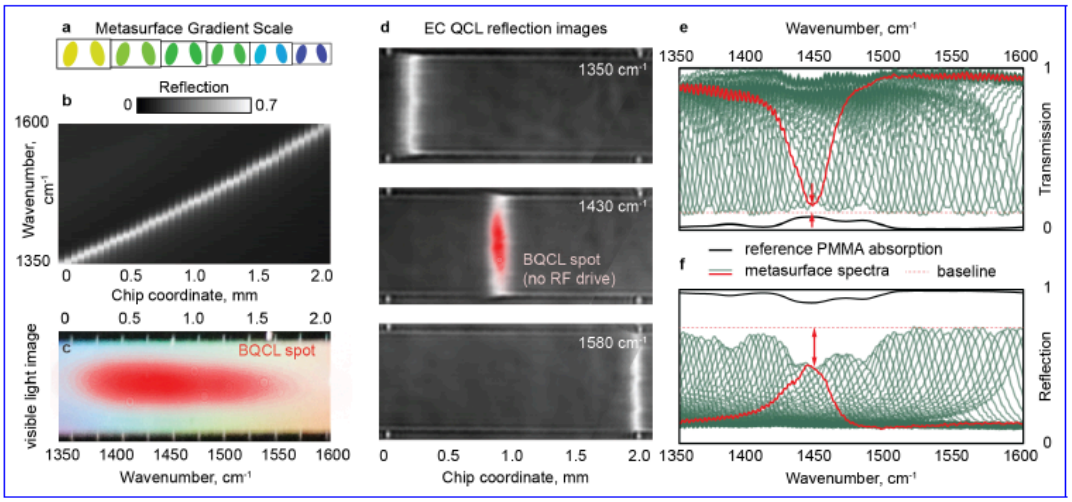

Figure 3 Broadband gradient metasurface for rapid SEIRA-based mid-IR imaging spectroscopy (a) Scheme of the unit cells of the resonance gradient metasurface consisting of two tilted Ge ellipses on CaF_2 substrate scaled along one of the chip coordinates. (b) Map of the reflection spectra of the gradient metasurface showing the evolution of the resonant peak with the chip coordinate. (c) Optical image of the gradient metasurface chip. Top axis shows the physical chip coordinate, bottom axis - the wavenumber of the resonant peak at the corresponding location on the chip. The red overlay shows the BQCL spot imaged with a mid-IR camera with the same scale (also shown in Fig. 2c). (d) Reflection images of the gradient metasurface chip measured at different excitation frequencies with ~~a mid-IR microscopy using external cavity tunable~~ commercial EC QCLs ~~as its light source~~setup (Daylight Solutions Spero). The overlay shows the intensity profile of the BQCL spot focused on the sample surface in single-frequency emission regime (no RF drive) and imaged in the same scale. (e) Stack of FTIR transmission spectra of the broadband resonance gradient metasurface covered with PMMA measured at different chip coordinates. ~~Polymer absorption has minor contribution~~ The spectrum indicated with red shows the strongest amplitude modulation compared to the ~~spectra~~ baseline metasurface transmission (indicated with ~~small red arrow~~horizontal dashed line). The magnitude of modulation is additionally illustrated with red arrows. (f) Stack of FTIR reflection spectra of the same chip. The amplitude of the peaks is strongly modulated by PMMA absorption~~(~~, with the most affected spectrum highlighted in red. The amplitude of modulation with respect to the baseline metasurface reflectivity (shown with dashed line) is indicated with red arrow~~)~~. Reference PMMA absorption profile is shown with black curves in both panels (inverted in panel f for convenience).

~~Unlike the mid-IR absorption spectra of analytes on CaF_2 chips that were detected in transmission , the metasurface-enhanced absorption signatures manifest much stronger in the reflection spectra. Figure 3e, f shows the comparison of~~ Molecular absorption enhanced by the resonant modes of the metasurface generally has different contributions to reflection and transmission signals. Either of the two channels can demonstrate stronger modulation depending on the metasurface design, as previous works demonstrated SEIRA both in reflection[18] and transmission[32] configurations. In our case, the metasurface design yields stronger modulation of reflectivity. We illustrate this by directly comparing transmission and reflection spectra measured from the gradient chip covered with a thin layer of PMMA ~~. The~~ (Figure 3e,f). While both the amplitudes of the transmission dips (Fig. 3e) and reflection peaks (Fig. 3f) are modulated by the absorption of PMMA, ~~its reference spectrum shown with black curves in both panels. The~~ the absolute modulation magnitude (indicated with red arrows in Fig. 3e,f) is almost six times stronger for reflection ~~. Therefore, to fully benefit from the absorption signal enhancement, we changed~~ (note that this does not represent the SEIRA enhancement factor, only its relative contribution to the signal collection channels). Therefore, SEIRA barcode measurements in our BQCL setup require switching of the detection scheme to reflection as illustrated in Fig. 4a to fully benefit from the signal enhancement.

- **Moreover, the comparison of transmission and reflection-based FTIR measurements in Figure 3e and f lacks meaning because the light path doubles in reflection mode. What is more concerning is that the authors derive conclusions in lines 168-169 stating 6-times signal enhancement. In the transmission mode measurements of PMMA in Figure 3e, metasurface resonance blocks light from reaching the FTIR detector, operating the instrument at its poor photon-starved state. The analyte absorbance signal interpretation collected in transmission mode on a reflective metasurface should not be used as a control to demonstrate the SEIRA effect.**

Following up on our response to the previous comment, the reported six-fold enhancement **does not represent the SEIRA effect**, and therefore the presented transmission data in Fig. 3e **is not a control experiment** that illustrates the absorption signature amplification. Figs. 3e and 3f compare two measurement configurations (transmission and reflection) of the same sample - PMMA layer deposited on the metasurface. This comparison justifies the use of reflection configuration in further measurements in Figs 4 and 5. The quantification of the SEIRA amplification and the appropriate control measurements are presented in Fig. 5. Please see our reasoning for the choice of the control measurements in the response to the next question.

ACTIONS TAKEN:
In the revised manuscript, we additionally specified that the reported six-fold difference in the absorption modulation does not represent SEIRA enhancement, but only relative contribution of the enhanced absorption signature to the two signal collection channels.

are modulated by the absorption of PMMA, ~~its reference spectrum shown with black curves in both panels. The~~ the absolute modulation magnitude (indicated with red arrows in Fig. 3e,f) is almost six times stronger for reflection ~~. Therefore, to fully benefit from the absorption signal enhancement, we changed~~ (note that this does not represent the SEIRA enhancement factor, only its relative contribution to the signal collection channels). Therefore, SEIRA barcode measurements in our BQCL setup require switching of the detection scheme to reflection as illustrated in Fig. 4a to fully benefit from the signal enhancement.

- **In Figure 5, where the authors quantify the SEIRA effect, they compare the absorption from the proposed laser-based setup with metasurfaces coated with polymer with that of gold mirror measurements on FTIR. This is not an acceptable way to compare signal amplification originating from metasurface resonances collected on two different substrates and instruments with distinct optical light-paths.**

We thank the reviewer for bringing up these points and allowing us to clarify the text better. Firstly, we would like to emphasize that SEIRA enhancement with dielectric metasurfaces is a well-established phenomenon that was quantified for similar structures in previous literature: Science 360 (6393), 1105-1109 (2018); Advanced Materials 36 (25), 2314279 (2024); Nature Nanotechnology 19 (12), 1804-1812 (2024). Importantly, the enhancement factor depends on the film thickness and strength of the vibrational mode involved; in particular, strong coupling effects influence the resulting signal amplification. While its quantification is not the focus of our manuscript, our detection principle, similarly to these previous works, relies on the modulation in resonant reflection of the metasurface. Naturally, the enhancement factors that we observe are consistent with the data reported in earlier works for films of similar thickness, in particular, ~80x factor enhancement for a PMMA film cf. Advanced Materials 36 (25), 2314279 (2024). It is important to note that the enhancement factor also depends on the absorption signature that is being detected, which is another manifestation of strong coupling effects.

We agree that using different instruments to extract the absorption signature can alter the quantification of the enhancement. However, a more important factor influencing the precision of the estimations is the low signal-to-noise ratio for absorption signals of thin films on bare substrates (which is the denominator used in the SEIRA enhancement factor calculation). In this context, we argue that the FTIR spectra of the polymer films on gold substrate that were used as a reference in our data are actually the optimal control measurement for two reasons:

1. The excitation geometry in FTIR measurements, performed using a Cassegrain objective, is almost identical to the imaging spectroscopy setup (~20 degrees angle of incidence defined by the aperture of the objective in case of FTIR and setup geometry in BQCL setup).
2. FTIR is more suitable for measurements of extremely weak absorption features of thin films without SEIRA enhancement, as the LN-cooled detector can compensate for the small signal magnitude with very long acquisition times. This is particularly important for accurate measurement of the value used in the denominator for enhancement factor calculation, thus crucial for accurate estimation of the SEIRA effect.

ACTIONS TAKEN:

We provided a justification for using FTIR data as a control measurement in the revised manuscript:

the corresponding normalized image. To accurately quantify the SEIRA effect, we measured the reference absorption spectra with FTIR for films of the same thickness deposited on a 150 nm gold film. In these measurements, we reproduced the excitation geometry of the BQCL setup by using a 35× Cassegrain objective that provides the same range of incidence angles (≈20 deg.). Making use of the long acquisition times available for FTIR (3 minutes for reference data in Fig. 5g-i), we improved the precision of the measurement of weak absorption of thin films without SEIRA enhancement, which would otherwise not be resolved in the single-shot data from BQCL. For polystyrene, which has the weakest absorption signature in the available

- **To prove their claims about the SEIRA based signal enhancement and the need for a gradient metasurface in the proposed optical configuration, the authors must compare their polymer layer coated metasurface measurements with the following controls on the same optical setup shown in Figure 4a: 1) by coating the diffraction grating with the same thickness of PMMA and extracting absorbance without the metasurface (or metasurface replaced with a gold mirror in Figure 4a). 2) by replacing the PMMA-coated metasurface with an Au mirror substrate coated with an identical thickness of PMMA and measuring spectra on the same setup Figure 4a). 3) In the setup in Figure 4a, keeping a bare metasurface in place and by inserting a PMMA coated CaF2 on the light path before the camera. Comparing measured spectra from these three control measurements with the PMMA coated metasurface and showing significant signal enhancement can prove the SEIRA effect in this setup.**

We thank the reviewer for suggestions on how to improve the control measurements. We would like to clarify that the quantification of SEIRA effect is not the main focus of this paper, as the performance of resonant dielectric metasurfaces for mid-IR absorption amplification has already been established in previous works. As we argue in detail in our response to the previous comment from the Reviewer (see above), the optimal controls are in fact based on FTIR measurements performed in the excitation geometry that correlates well with our BQCL imaging setup (reflection with ~20 degrees angle of incidence for both), and they provide sufficient evidence of the SEIRA effect. The consistency of our data with estimations of the amplification factor in previous literature (e.g. Advanced Materials 36 (25), 2314279 (2024)) further support our claims.

We also want to note that coating our commercial diffraction grating with PMMA (option 1 of the Reviewer) is not a feasible approach, because its form-factor is incompatible with spin-coating and also the cleaning procedures would eventually damage its optically delicate surface. As for the absorption measurements of thin films without SEIRA enhancement using our BQCL imaging setup (options 2,3 of the Reviewer), the noise level of the single-shot measurements with our low-cost and room temperature camera as well as the minor imaging artifacts that are discussed in the main manuscript prevent an accurate estimation of the small denominator value of SEIRA enhancement factor. To illustrate this, we present below the reflectivity image of a gold film covered with 80 nm PMMA normalized to reflection

of clean gold film measured with BQCL setup, which shows no prominent absorption features that can be reliably used for estimations.
Overall, this further supports that SEIRA effect provided by our gradient metasurface is indeed necessary for fast detection of absorption signatures in the broadband imaging configuration.

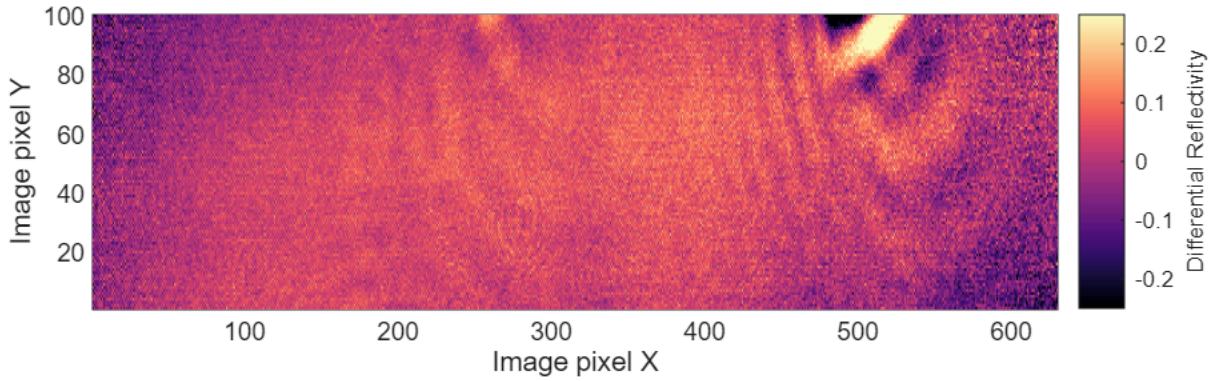

Figure R1. Reflection image from a gold film covered with 80 nm PMMA normalized to reflection form a clean fold film.

ACTIONS TAKEN:
The revised manuscript now provides a detailed justification of using FTIR data as a control measurement:

volume. ~~Accordingly~~To illustrate this, we used different thicknesses of molecular layers ~~for extraction of metasurface-enhanced absorption barcodes and compared their profile with reference absorption data extracted from FTIR reflectance spectra of films deposited on gold (see Methods for details on the measurement configuration)~~in our experiments. The absorption spectra (Fig. 5g-i) were extracted from the normalized images (Fig. 5d-f) as $A = R_{\text{bare}} - R_{\text{barcode}}$, where R_{bare} stands for the average reflectivity profile of the bare metasurface measured once at the calibration stage (Fig. 4e), and R_{barcode} stands for the vertically averaged reflectivity profile of the corresponding normalized image. To accurately quantify the SEIRA effect, we measured the reference absorption spectra with FTIR for films of the same thickness deposited on a 150 nm gold film. In these measurements, we reproduced the excitation geometry of the BQCL setup by using a 35× Cassegrain objective that provides the same range of incidence angles (≈20 deg.). Making use of the long acquisition times available for FTIR (3 minutes for reference data in Fig. 5g-i), we improved the precision of the measurement of weak absorption of thin films without SEIRA enhancement, which would otherwise not be resolved in the single-shot data from BQCL. For polystyrene, which has the weakest absorption signature in the available

- **The methods for the fabrication of the metasurface are not sufficient for the readers to reproduce the results. Clarifications are needed on why an inverted pattern was exposed using EBL instead of using a negative resist or a positive resist with a hard mask to etch Ge. Also, details on Ge etching recipe (gas type, flow rate, plasma power) need to be included.**

We thank the reviewer for pointing out the insufficient details and allowing us to improve the text. Inverted pattern was used to improve on the quality factor of the resonances and

significantly reduce the fabrication cost. Direct e-beam resist patterning requires the use of a hard mask and the associated lift-off process. The commonly used alumina mask cannot be removed without damaging the underlying germanium, and its absorption increases towards the longer wavelengths of the mid-IR range. Furthermore, to ensure its effective lift-off, costly long-throw evaporation processes are needed; furthermore, oxides contaminate the evaporation chamber and require frequent cleaning, which limits the tool availability. In our approach, we exclude this step from the process flow thus reducing the fabrication time drastically.
At the same time, the fill-factor of the unit cell design is close to 50%, which means that exposure time for inverted and non-inverted patterns is similar. Therefore, there is no incentive to use more expensive and difficult to handle negative tone resists.
Following the Reviewer's advice, we added additional details on the Ge etching recipe to the methods section.

ACTIONS TAKEN:
We revised the Methods section to include the justification of using the inverted design approach as well as etching parameters requested by the reviewer. The related subsection of Methods now reads:

Metasurface fabrication

Gradient metasurfaces based on germanium (Ge) resonators were fabricated on calcium difluoride (CaF_2) substrates. First, the material stack was prepared by subsequent sputtering of a 5 nm silicon oxide (SiO_2) adhesion layer and a 700 nm Ge layer on top of a 1 mm thick CaF_2 chip. ~~The inverted metasurface pattern was~~ To exclude the absorption from the alumina hard mask that is usually used for patterning of Ge films, we used an inverted metasurface exposure pattern, written using electron beam lithography (Raith EPBG500+) on a spin-coated single-layer PMMA (PMMA 495k A8, 4000 rpm) positive tone resist. After the development, the pattern was directly transferred to the Ge film using a continuous fluorine-based dry plasma etching process (Alcatel AMS 200 SE, 1500 W SF_6/C_4F_8 plasma at 25/55 sccm flow; temperature of the chuck 20°C). To suppress the defects arising from stitching errors of the neighboring write fields of the e-beam tool, we additionally customized the e-beam exposure sequence to follow a meander path in column-by-column fashion. For reflection references used to produce the data in Fig. 5, 150 nm gold film was deposited on the unetched Ge/CaF_2 substrate with magnetron sputtering (Alliance-Concept DP 650).

Reviewer #3 (Remarks to the Author):

The paper reports on an advanced SEIRA technique with pronouncedly reduced acquisition time. Such a breaking result was obtained with the use of a few crucial improvements in the experimental method. First, a quantum cascade laser with radio-frequency modulation provides a broadband coherent source for mid-IR spectrometry. Second, a metasurface helps to enhance the response. Third, the gradient variation of the lattice constant of the metasurface elements allows for achieving a frequency range translation in the coordinate space. All these actions lead to an extremely short time of the Mid-IR acquisition, validated experimentally with reasonable accuracy. Thus, the paper, which presents a novel trustworthy experimental spectroscopy technique, warrants publication. However, there are a few points that require attention to better convey the results to the auditorium.

We thank the reviewer for positive assessment of the novelty of our approach and highlighting the importance of our achievement for **an extremely short time of the Mid-IR acquisition**.

1. It is not clear how the absorption spectra were extracted, taking into account that reflection is measured in the range of 0 to 0.6. Is it simply the reflection of a bare metasurface minus the reflection of a metasurface coated with an analyte layer? Did the analyte coating happen from the substrate part or on top of the metasurface elements? What about the analytes' profile then? It will be nice to provide a more detailed description of the retrieval of infrared absorption.

We thank the reviewer for these useful suggestions. The barcode images in Fig. 5d-f are obtained by normalizing a reflection image from a metasurface covered with a respective analyte by a reflection image of a gold film in the same measurement configuration. In this scenario, we are extracting the absolute modulation of the signal, which is necessary for quantitative estimation of the absorption signal, as well as its enhancement as compared to thin films on unstructured substrates. We note that the original Fig. 5 contained an inconsistency of the units in the FTIR data (panels a-c) and the barcode images (absolute reflectivity). We have revised Figure 5a-c and plotted the respective data in the absolute units of reflectivity.

The coating procedure is detailed in the methods section. Alanine deposition is performed with thermal evaporation with short target-to-sample distance. Both PMMA and PS are deposited using spin-coating. While the exact coating profile is challenging to extract, our experience from previous works that studied the thickness dependence in more detail (Advanced Materials 36 (25), 2314279 (2024)) shows that the film thickness extracted from AFM data on flat substrates is a good approximation.

ACTIONS TAKEN:
Following the reviewer's advice, we complemented the revised manuscript with a detailed explanation of the retrieval of the absorption signal for Fig.5 d-f:

As revealed by the ~~FTIR spectra~~ spatially resolved metasurface reflectivity spectra stacks measured with FTIR (Fig. 5a-c), the presence of analytes modifies the reflectance of the gradient metasurface at the locations where the metasurface resonance matches the absorption peaks. Illumination of the gradient chip with the diffraction spot of our BQCL converts this spatially encoded absorption into a "barcode" image defined by the absorption signature of the corresponding molecule. ~~This molecular absoprtion barcode can be captured~~ We capture this molecular absorption barcode in a single frame of a mid-IR imaging camera, ~~providing~~ thus realizing rapid identification of the analyte. The images captured for three analytes ~~and normalized to reflection from gold film~~ are shown in Fig. 5d-f. Each image is normalized to reflection from a 150 nm gold film evaporated on a reference area of the chip through a mask (see Methods). One can immediately see the pronounced reflection minima ~~corresponding to~~ that match the absorption resonances of the respective molecules ~~that~~ and manifest as dark vertical stripes in the images. ~~The line defects visible in the images come from the stitching~~ Notably, the barcode images contain several types of artifacts that contribute to the extracted absorption spectra. First, stitching errors

And Fig. 5g-i:

volume. ~~Accordingly~~To illustrate this, we used different thicknesses of molecular layers ~~for extraction of metasurface-enhanced absorption barcodes and compared their profile with reference absorption data extracted from FTIR reflectance spectra of films deposited on gold (see Methods for details on the measurement configuration)~~in our experiments. The absorption spectra (Fig. 5g-i) were extracted from the normalized images (Fig. 5d-f) as $A = R_{\text{bare}} - R_{\text{barcode}}$, where R_{bare} stands for the average reflectivity profile of the bare metasurface measured once at the calibration stage (Fig. 4e), and R_{barcode} stands for the vertically averaged reflectivity profile of the corresponding normalized image. To accurately quantify the SEIRA effect, we

2. The small red arrow in Fig.3e is hardly visible, however, the clearly seen red curve is not explained in the Caption.

We thank the reviewer for noticing this omission. In the revised manuscript, the caption now indicates the meaning of the red curve highlight. In addition, the red arrow is made more visible.

ACTIONS TAKEN:

We revised Fig. 3 and its caption to address the missing information and element visibility issues:

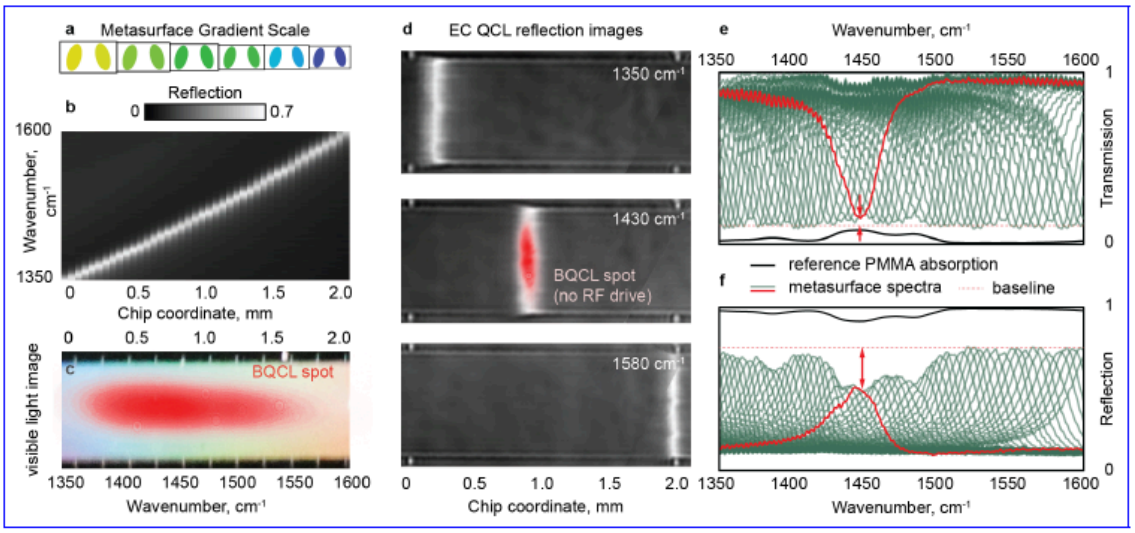

Figure 3 Broadband gradient metasurface for rapid SEIRA-based mid-IR imaging spectroscopy (a) Scheme of the unit cells of the resonance gradient metasurface consisting of two tilted Ge ellipses on CaF_2 substrate scaled along one of the chip coordinates. (b) Map of the reflection spectra of the gradient metasurface showing the evolution of the resonant peak with the chip coordinate. (c) Optical image of the gradient metasurface chip. Top axis shows the physical chip coordinate, bottom axis - the wavenumber of the resonant peak at the corresponding location on the chip. The red overlay shows the BQCL spot imaged with a mid-IR camera with the same scale (also shown in Fig. 2c). (d) Reflection images of the gradient metasurface chip measured at different excitation frequencies with ~~a mid-IR microscopy using external cavity tunable~~ commercial EC QCLs ~~as its light source~~setup (Daylight Solutions Spero). The overlay shows the intensity profile of the BQCL spot focused on the sample surface in single-frequency emission regime (no RF drive) and imaged in the same scale. (e) Stack of FTIR transmission spectra of the broadband resonance gradient metasurface covered with PMMA measured at different chip coordinates. ~~Polymer absorption has minor contribution~~ The spectrum indicated with red shows the strongest amplitude modulation compared to the ~~spectra~~ baseline metasurface transmission (indicated with ~~small red arrow~~horizontal dashed line). The magnitude of modulation is additionally illustrated with red arrows. (f) Stack of FTIR reflection spectra of the same chip. The amplitude of the peaks is strongly modulated by PMMA absorption~~(~~, with the most affected spectrum highlighted in red. The amplitude of modulation with respect to the baseline metasurface reflectivity (shown with dashed line) is indicated with red arrow~~)~~. Reference PMMA absorption profile is shown with black curves in both panels (inverted in panel f for convenience).

3. It is worth showing the main fingerprints of the analyte vibration bands used for the method characterisation directly in Fig.5d-i (also Fig.2d,e) but not referring to them in the bold text.

We thank the reviewer for bringing up this point and giving us the opportunity to improve the Figures. The schematics of the molecules that are introduced in Fig. 2d,e and Fig. 5d-f were added for a better visual attribution of the data to a specific analyte. The schematic thus serves as a guide for the eye. As suggested, we highlighted the main fingerprints of the analyte vibration bands in Fig 2d.e (not included in Fig.5 which is already busy with other details).

ACTIONS TAKEN:

We Revised Fig. 2d,e to show the main fingerprints of the analyte vibration bands.

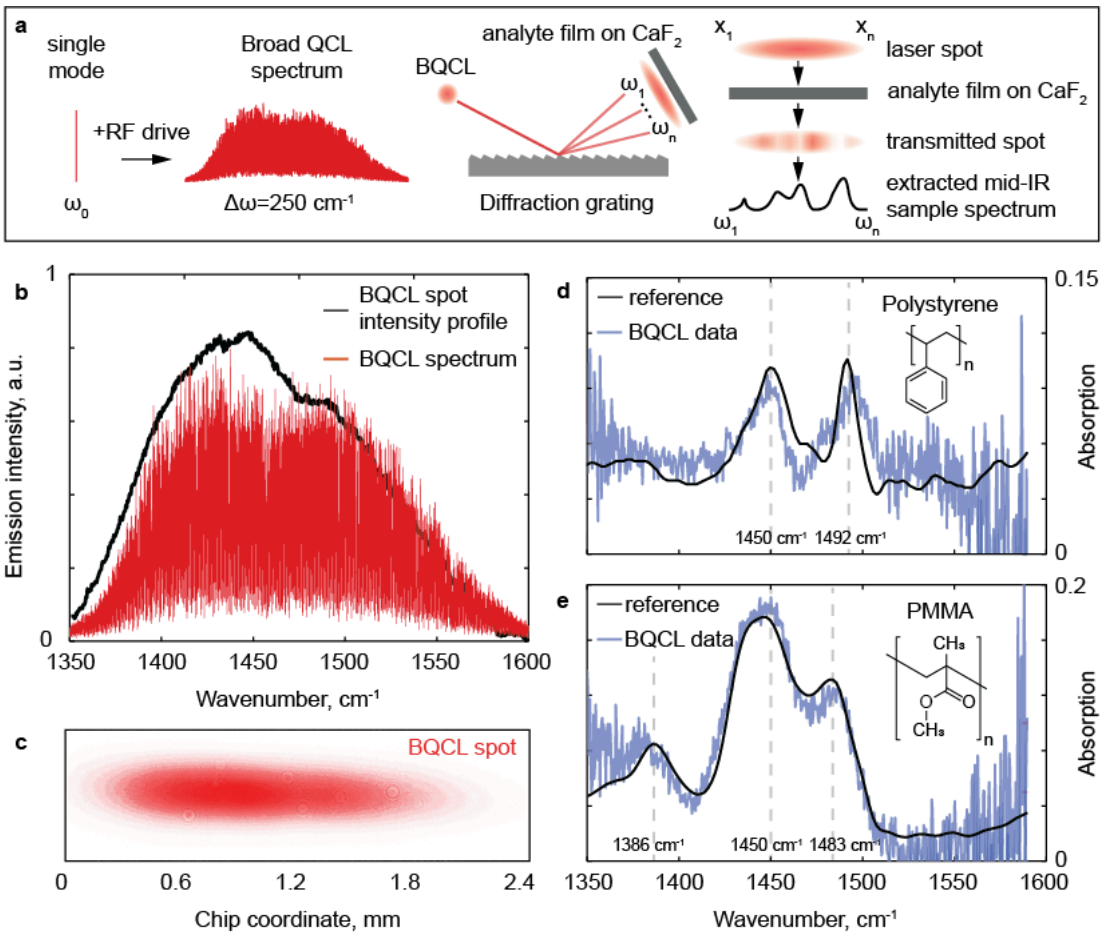

4. Have the FTIR spectra in Fig.2d,e, error bars, or are they too small to be seen? Should be commented.

We thank the reviewer for this comment. The FTIR data was accumulated over many scans for a total acquisition time of 2 minutes and additionally smoothed to improve the visibility of the BQCL data.

ACTIONS TAKEN:

We revised the text to explicitly mention the averaging procedure in the Figure 2 caption. Furthermore, to outline the conditions where our detection method outperforms the FTIR, we added a new Supplementary Figure S2 which shows the noise level of the data measured with BQCL setup and FTIR for different signal accumulation times.

Figure 2 ~~Imaging spectroscopy with broadband quantum cascade laser~~ Principle of non-enhanced imaging spectroscopy with broadband quantum cascade laser (a) Schematic of the broadband QCL imaging spectroscopy components. Left: quantum cascade laser is driven into broadband emission regime using radiofrequency drive. Center: broadband laser emission is projected on a sample surface through a dispersive element and then imaged with a mid-IR camera. Right: as each frequency component of BQCL addresses a specific coordinate on the sample surface, the spatial profile of the laser spot represents the sample transmission spectrum~~that can be extracted from a single frame of a mid-IR imaging camera~~. (b) Spatial intensity profile of a projected laser spot (black curve) compared to the spectrum of BQCL emission measured with FTIR (red curve). (c) Image of the BQCL spot on the surface of CaF_2 chip recorded with a mid-IR camera. (d,e) Comparison of the absorption spectra of (d) polystyrene and (e) polymetylmetacrylate films on CaF_2 measured with FTIR (black curves, smoothed using a 20-point moving average) and extracted from the spatial intensity profiles of the transmitted BQCL beam (~~red~~ blue curves).

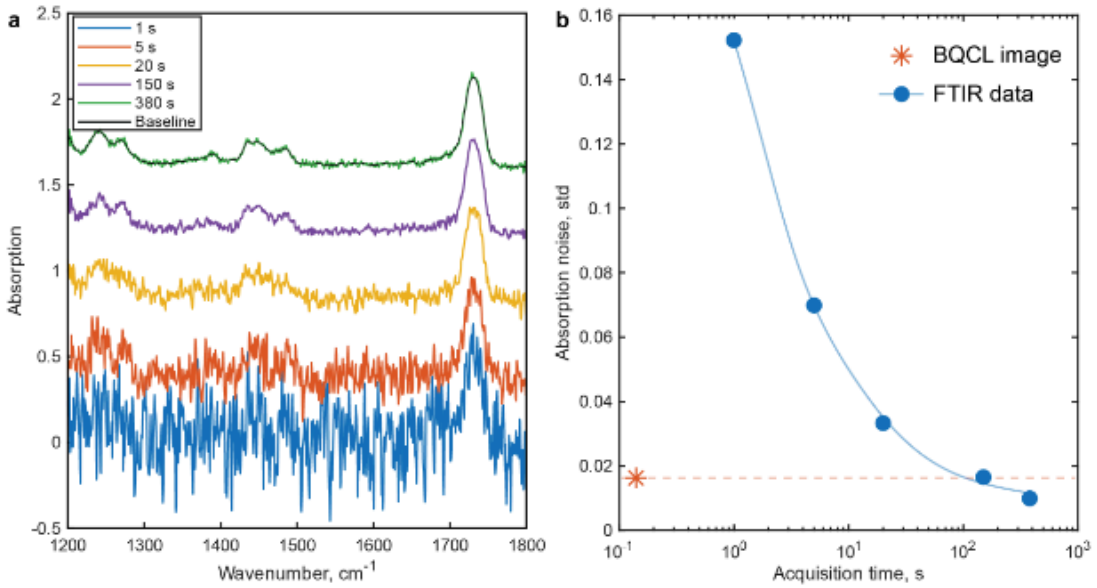

Figure S2: **a**, Absorption spectra of 800 nm PMMA layer on CaF_2 chip measured for different acquisition time (number of averages), illustrating the reduction of noise level with longer measurement. Each consecutive spectrum is shifted vertically by 0.4 to facilitate the comparison. **b**, Dependence of the noise level calculated as the standard deviation from the absorption baseline (shown with black curve on top of 380 s spectrum in panel a).

5. While blue and red curves in Fig.5g-i are matching pretty well in the range1425 -1500 cm^-1, QCL SEIRA provides additional features beyond this range. These features are not supported by FTIR measurement despite its very small errors according to the calibration in Fig.2. Are there any explanations?

We thank the reviewer for pointing out this issue. The artifacts at the shorter wavelength (larger wavenumber) edge of the spectrum shorter are related to the aberrations that emerge in the reflection configuration due to a longer path length and consequently larger divergence of the laser beam in this configuration. These artifacts are visible also in the calibration image (Fig. 4d). We expect that this issue can be resolved with a larger size of the imaging lens, which was unavailable at the time of the experiment.
The artifact at the longer wavelength edge of the spectrum in Fig. 5g is related to the stray particle in the spin coated layer of polystyrene that introduces additional scattering (visible also in barcode image in Fig. 5d). Generally, we found polystyrene spin-coating more

challenging due to lower viscosity of the solvent (o-xylene) and considerable number of particles naturally occurring in the solution prepared from commercial PS.

ACTIONS TAKEN:

We added the discussion mentioning the origin of the artifacts in reflection configuration as well as a discussion on mitigation strategies.

~~that~~ and manifest as dark vertical stripes in the images. ~~The line defects visible in the images come from the stitching~~ Notably, the barcode images contain several types of artifacts that contribute to the extracted absorption spectra. First, stitching errors of the write fields of the e-beam tool ~~. However,~~ lead to additional light scattering, which is visible as minor line defects in the images. Second, the analyte deposition process sometimes produces small particles on the chip surface, one of which is visible in the smaller wavenumber range in Fig. 5d. Finally, the difference of the path length of the BQCL spectral components in reflection geometry induces aberrations towards larger wavenumbers (¿1525 cm^{-1}), which are also visible in the calibration image in Fig. 4e. In our showcase, these artifacts do not interfere with the ~~strongly pronounced absorption features~~detected absorption features, but potentially can be mitigated by using large-scale fabrication approaches such as deep-UV lithography and by introducing custom aberration compensation in the optical setup.

Reviewer #1 (Remarks to the Author):

I thank the authors for clarifying the advantages of their laser source in the context of infrared spectroscopy. With these revisions, the manuscript now positions its contribution more clearly within the field. I would still encourage the authors to avoid potentially exaggerated wording such as "... remarkably broad ..." and instead adopt more objective and quantitative language throughout the text.

Our response:

We greatly appreciate the Reviewer's positive feedback on the revised manuscript and his/her extremely useful comments and suggestions that allowed us to improve the paper and context of our results. Following the Reviewer's advice, we removed the subjective and/or exaggerated wording from the latest revision of the manuscript.

Given that the principal strength of the proposed method appears to be its acquisition speed (reported to be approximately three orders of magnitude faster than FTIR), it would be valuable for the authors to discuss in more detail which sensing or spectroscopy applications critically benefit from such speed. Highlighting specific use cases where this performance advantage is essential would further strengthen the motivation and impact of the work.

Our response:

We thank the Reviewer for useful suggestion. We added a discussion on the application cases for rapid mid-IR detection to the final section of the paper:

for FTIR-based spectroscopy techniques. We envision that our approach will facilitate rapid and highly specific molecular diagnostics across a wide range of chemical and biological applications and inspire the development of highly compact and minaturized mid-IR bioanalytical devices. In particular, the platform offers significant potential for applications that require continuous monitoring, including the inspection of surface organic residues and polymer coatings, as well as the monitoring of surface reactions.

Reviewer #3 (Remarks to the Author):

The reviewer's comments elicited a quite verbose response letter with intensive discussions on many important points. The answers and changes made in the revised manuscript definitely improve the quality and readability of the paper and the trustworthiness of the presented results. The paper warrants publication in the journal.

Our response:

We greatly appreciate the Reviewer's contribution to the review process.